

AIAA 81-0280R

# Thermodynamic Equilibrium-Air Correlations for Flowfield Applications

E. V. Zoby\* and J. N. Moss†  
NASA Langley Research Center, Hampton, Va.

Equilibrium-air thermodynamic correlations have been developed for flowfield calculation procedures. A comparison between the postshock results computed by the correlation equations and detailed chemistry calculations is very good. The thermodynamic correlations are incorporated in an approximate inviscid flowfield code with a convective heating capability for the purpose of defining the thermodynamic environment through the shock layer. Comparisons of heating rates computed by the approximate code and a viscous-shock-layer method are good. In addition to presenting the thermodynamic correlations, the impact of several viscosity models on the convective heat transfer is demonstrated.

## Nomenclature

$a_i, b_i$	= least squares coefficients
$c_1, c_2, c_3, c_4, c_5$	= defined by Eqs. (19-23)
$C_f$	= skin friction
$C_h$	= enthalpy coefficient [Eq. (1)]
$C_T$	= temperature coefficient [Eq. (2)]
$h$	= enthalpy
$\bar{h}$	= nondimensional enthalpy = $h/RT_0$
$K$	= defined by Eq. (12)
$M$	= order of least-squares polynomial
$m, n, \ell, k$	= exponents [Eqs. (1) and (2)]
$N$	= reciprocal exponent in velocity profile power law
$p$	= pressure
$p_0$	= pressure at standard conditions = 1 atm
$\bar{p}$	= nondimensional pressure = $p/p_0$
$Pr$	= Prandtl number
$q$	= defined by Eq. (18)
$\dot{q}_c$	= convective heating rate
$R$	= gas constant for air based on molecular weight of 28.92
$R_N$	= body nose radius
$R_\theta$	= momentum-thickness Reynolds number
$r$	= radius of body of revolution
$s$	= surface wetted distance
$T$	= temperature
$T_0$	= temperature at standard conditions = 273 K
$\bar{T}$	= nondimensional temperature = $T/T_0$
$U$	= velocity
$U_h$	= transformed velocity for enthalpy correlation [Eqs. (3) and (5)]
$U_T$	= transformed velocity for temperature correlation [Eqs. (4) and (7)]
$Y$	= distance normal to wall
$\delta$	= boundary-layer thickness
$\delta^*$	= displacement thickness
$\theta$	= momentum thickness
$\theta_c$	= cone half-angle
$\theta_s$	= shock angle

$\mu$	= viscosity
$\rho$	= density
$\rho_0$	= density at standard conditions = 1.292 kg/m <sup>3</sup>
$\bar{\rho}$	= nondimensional density = $\rho/\rho_0$

## Subscripts and Superscripts

$aw$	= adiabatic wall
$e$	= edge conditions
$2$	= conditions immediately behind shock
$*$	= conditions determined by reference enthalpy
$\infty$	= freestream conditions
$L$	= laminar
$s$	= stagnation-point conditions
$t$	= turbulent
$w$	= wall

## Introduction

ACCURATE evaluation of the aerodynamic heating rates is essential to the proper design of most entry vehicles. Viscous-shock-layer (VSL) analyses<sup>1,2</sup> provide a direct means for computing these radiative and convective heat fluxes as well as any interactions between inviscid and viscous flow regions due to heat transfer, entropy-layer swallowing, and mass injection. VSL methods eliminate the need of an iterative boundary-layer, inviscid-flow solution since the VSL governing equations are uniformly valid through the shock layer. However, VSL methods require large computer run times and storage; consequently, such solution techniques are expensive to run and are not generally applicable to parametric studies or design calculations. Thus VSL methods serve usually as "benchmark" solutions while engineering heating methods,<sup>3-12</sup> which have been substantiated by experimental data and/or "benchmark" calculations, are employed in parametric or design calculations.

One aspect of the benchmark codes that consumes an appreciable amount of computer storage and computational time is the complex equilibrium code for calculating the thermodynamic and transport properties. Obviously, it would not be advantageous to include detailed chemistry codes in the approximate heating analyses. Hence, correlation equations<sup>13-17</sup> based on results of detailed calculations are incorporated in engineering analyses for computing the thermodynamic environment about entry vehicles. Such correlation equations, applicable to hydrogen-helium gas mixtures,<sup>17</sup> were incorporated recently in an approximate flowfield code, which was demonstrated to provide rapid and

Presented as Paper 81-0280 at the AIAA 19th Aerospace Sciences Meeting, St. Louis, Mo., Jan. 12-15, 1981; submitted April 22, 1981; revision received Nov. 4, 1981. This paper is declared a work of the U.S. Government and therefore is in the public domain.

\*Aero-Space Technologist, Aerothermodynamics Branch, Space Systems Division. Member AIAA.

†Research Leader, Aerothermodynamics Branch, Space Systems Division. Member AIAA.

reliable predictions for the radiative and convective heat-transfer rates about probes entering the atmospheres of the outer planets.<sup>12,18</sup> Transport property correlations<sup>19</sup> based on detailed transport property calculations that employ the complete kinetic-theory formulas for transport analysis were used in the engineering heat-transfer predictions.

As a result of the usual ballistic entries, the pending Shuttle flights, and an increasing interest in advanced transportation systems, an approximate flowfield analysis similar to the planetary code should be advantageous for engineering heat-transfer predictions at Earth entry conditions. The purpose of this paper is to present equilibrium-air thermodynamic correlations that can be incorporated simply into that code. Transport correlations similar to those used in the planetary studies<sup>19</sup> are not presented since detailed transport calculations for equilibrium air are not currently available. Actually, it is difficult to evaluate the adequacy of even the existing transport models.<sup>20-24</sup> The detailed equilibrium-air, normal-shock properties of Lewis and Burgess<sup>25</sup> have been used as the basis to develop the present thermodynamic correlations. The correlation equations are applicable over a range of freestream velocities from 1.829 to 7.925 km/s and freestream pressures from  $2.0 \times 10^{-5}$  to  $1.0 \times 10^{-1}$  atm.

The correlation equations as well as the methods used to develop the correlations are reported herein. Thermodynamic properties computed by the correlation equations, coupled with the shock equations, are validated by comparison with results computed by detailed equilibrium-air shock calculations.<sup>25-27</sup> The thermodynamic correlations are incorporated in an approximate inviscid-flowfield method with a convective heating-rate capability. Heating rates computed with this engineering method are compared with corresponding VSL calculations at Earth entry conditions. Also, a quantitative assessment of the impact of several sets of viscosity models on the convective heat transfer is presented.

### Analysis

This section presents the procedures used to develop the equilibrium-air thermodynamic correlations as well as the resulting equations. The thermodynamic correlations are incorporated in an approximate inviscid-flowfield code with a convective heating capability. Thus the heat-transfer equations are presented also in this section.

### Thermodynamic Correlations

For the enthalpy and temperature, equations of the form

$$\bar{h} = C_h \bar{p}^m / \bar{\rho}^n \quad (1)$$

and

$$\bar{T} = C_T \bar{p}^l / \bar{\rho}^k \quad (2)$$

have been developed<sup>17</sup> to calculate the thermodynamic properties in hydrogen-helium gas mixtures and were shown

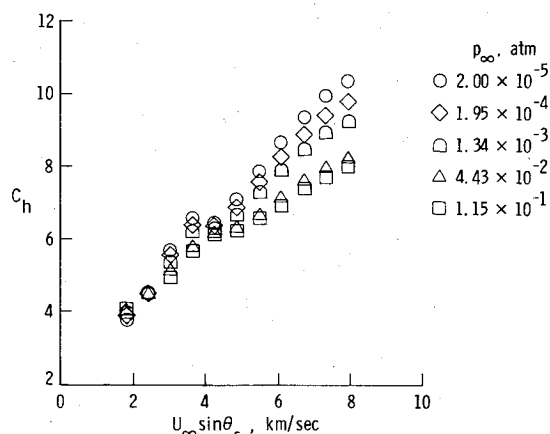


Fig. 1 Enthalpy proportionality constants for shock solutions.

to provide a rapid, but reliable, method of computing the properties. The results of this previous study demonstrated that by evaluating the proportionality constants,  $C_h$  and  $C_T$ , at postshock conditions and correlating these values as a function of the freestream velocity and shock angle, satisfactory comparisons of calculated shock properties based on the approximate correlations and on detailed chemistry codes were obtained. Note that such thermodynamic correlations have been incorporated in an approximate inviscid-flowfield method for calculating local shock-layer properties.<sup>12,18</sup>

Similar correlation techniques for the thermodynamic properties have been used herein at Earth entry conditions. Thus the present thermodynamic correlations are applicable only to flowfield calculations. The correlations are based on the equilibrium-air, normal-shock properties of Lewis and Burgess<sup>25</sup> and are developed over a range of freestream velocities from 1.829 to 7.925 km/s and freestream pressures from  $2.0 \times 10^{-5}$  to  $1.0 \times 10^{-1}$  atm. For this range of conditions, values of  $C_h$  and  $C_T$  were calculated from Eqs. (1) and (2) for known normal-shock properties and values of the exponents  $m$ ,  $n$ ,  $l$ , and  $k$  equal to 0.97, 0.98, 0.70, and 0.68, respectively. The values of the exponents were selected based on prior experience in developing these correlation equations and results presented in Refs. 13-17.

The trends of  $C_h$  as well as the  $C_T$  curves for the assumed freestream conditions were observed<sup>28</sup> to be similar. A shift of these curves was performed whereby the curves representing different freestream pressures were collapsed to the curve for  $p_\infty = 2.0 \times 10^{-5}$  atm, thus yielding a single curve. The collapsing procedure required a shift of the curves along the abscissa for  $C_h$  and along the ordinate for  $C_T$ . The results of these calculations are demonstrated in Ref. 28. As an illustration of this procedure for this paper, the calculation of the  $C_h$  term and subsequent transformation to a single curve are shown in Figs. 1 and 2, respectively. The terms  $C_h^*$  and  $C_T^*$  represent the values of  $C_h$  and  $C_T$  after the collapsing process and can be written in terms of normalized parameters  $U_h$  and  $U_T$ , respectively, as

$$C_h^* = \sum_{i=1}^M a_i U_h^{i-1} \quad (3)$$

and

$$C_T^* = \sum_{i=1}^M b_i U_T^{i-1} \quad (4)$$

The transformed data were curve fitted by a tenth-order, least-squares polynomial for  $C_h^*$  and an eleventh-order, least-squares polynomial for  $C_T^*$ . The coefficients for the least-squares polynomials applicable to  $C_h^*$  and  $C_T^*$  are given in

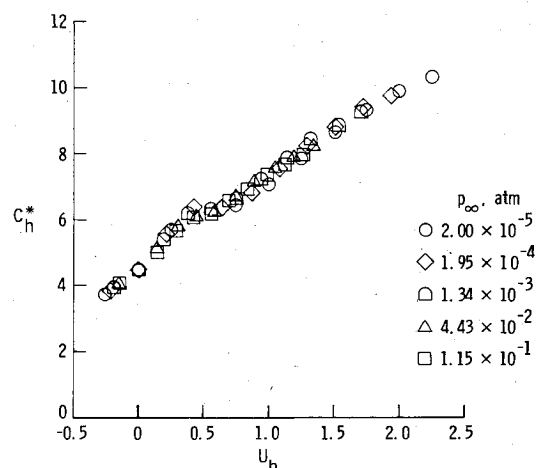


Fig. 2 Transformed enthalpy proportionality constants.

**Table 1** Least-squares coefficients for transformed enthalpy and temperature proportionality constants

<sup>a</sup> Transformed enthalpy proportionality constant		<sup>b</sup> Transformed temperature proportionality constant	
$C_h^* = \sum_{i=1}^M a_i U_h^{i-1}$		$C_T^* = \sum_{i=1}^M b_i U_T^{i-1}$	
$a_1$	4.529228633899	$b_1$	12.297991101529
$a_2$	4.476970720900	$b_2$	-8.238094255731
$a_3$	1.38655275431	$b_3$	2.419592541157
$a_4$	-13.142746144615	$b_4$	-0.335380942364
$a_5$	6.997767376225	$b_5$	0.02067595608575
$a_6$	21.914473834036	$b_6$	0.0001046732310838
$a_7$	-34.236435659858	$b_7$	-0.0001014180246941
$a_8$	20.407570958029	$b_8$	0.6888281850264E-05
$a_9$	-5.668335244460	$b_9$	-0.2245678457584E-06
$a_{10}$	0.611030863675	$b_{10}$	0.3725350878072E-08
		$b_{11}$	-0.2518960222376E-10

Table 1. (The user is cautioned that such high-order polynomial curve fits are not applicable usually outside the correlation range.) The value of  $U_h$  in Eq. (3) is given by

$$U_h = A (U_\infty \sin \theta_s - 2.4384) / 2.4384 \quad (5)$$

where

$$A = \exp[\ln(2.0 \times 10^{-5} / p_\infty) / 15.0] \quad (6)$$

Also, the value of  $U_T$  in Eq. (4) is given by

$$U_T = U_\infty \sin \theta_s / 0.3048 \quad (7)$$

Thus the values of  $C_h$  and  $C_T$  can be computed for a specified freestream velocity (km/s), freestream pressure (atm), and shock angle by using Eqs. (3-7) in conjunction with the appropriate polynomial coefficients and the relations

$$C_h = C_h^* \quad (8)$$

and

$$C_T = C_T^* / e^{C \cdot B} \quad (9)$$

where

$$C = [(U_T - 20.0) / 18.0] \{ [(U_T - 12.0) / 12.0]^2 \}^{0.05} \quad (10)$$

and

$$B = \ln(2.0 \times 10^{-5} / p_\infty) / 50.0 \quad (11)$$

For convenience, a brief outline for the application of the correlation methods is given as follows:

1) Given freestream pressure and velocity as well as  $\theta_s$  and appropriate polynomial coefficients, compute  $U_h$  and  $C_h^*$  from Eqs. (5) and (3), respectively.

2) Compute  $C_h$  from Eq. (8).

3) With the equation given for  $\bar{h}$  [Eq. (1)], an equation of state in the form of  $h = h(p, \rho)$  has been obtained.

4) Shock properties for enthalpy, pressure, and density can be computed with the oblique-shock relations and equation of state from step 3. The corresponding temperature may then be computed with Eqs. (4), (7), and (9), and the equation for  $\bar{T}$ .

#### Approximate Heating Relations

Laminar and turbulent heating-rate equations appropriate for engineering predictions of the convective heating rates about blunt re-entry spacecraft at hypersonic conditions were reported recently.<sup>11</sup> The appropriate methods were demonstrated to be applicable to both perfect and equilibrium

gas mixtures for either constant or variable-entropy edge conditions. The equations are repeated herein for completeness. A brief review of why the particular equations were selected is also included.

For the stagnation-point, heat-transfer calculations, the equation of Sutton and Graves<sup>3</sup>

$$\dot{q}_{w,s} = K(p_s / R_N)^{1/2} (h_s - h_w) \quad (12)$$

is used. Stagnation-point, heat-transfer results computed with Eq. (12) are in good agreement with results computed by the Cohen method<sup>5</sup> at equilibrium-air conditions. Since the constant  $K$  in Eq. (12) can be determined by a simple but accurate method over a wide range of gas mixtures and is simple to program, the method of Sutton and Graves<sup>3</sup> is used in the approximate flowfield analysis rather than the more widely recognized Cohen<sup>5</sup> method.

The laminar heat-transfer distributions are computed by relating heat transfer to a skin-friction relation based on  $R_\theta$  through a modified form of Reynolds analogy. This approach was used in Ref. 11, since existing laminar heating methods are not applicable over a wide range of gas mixtures. The approach is useful for approximating the variable-entropy effects on the heat-transfer calculations and is used also in this investigation. The laminar heat transfer is computed using a standard incompressible skin-friction relation with compressibility effects accounted for by Eckert's reference-enthalpy relation<sup>29</sup> and is given by

$$\dot{q}_{w,L} = 0.22 (R_{\theta,e})^{-1} (\rho^* / \rho_e) (\mu^* / \mu_e) \rho_e U_e \times (h_{aw} - h_w) (Pr_w)^{-0.6} \quad (13)$$

where  $\theta$  is computed by

$$\theta_L = 0.644 \left( \int_0^s \rho^* \mu^* U_e r^2 ds \right)^{1/2} / (\rho_e U_e r) \quad (14)$$

The turbulent heat transfer is also computed by relating heat transfer to a skin-friction relation based on  $R_\theta$  through a modified form of Reynolds analogy. The skin-friction relation is determined by assuming a velocity profile,  $U/U_e = (Y/\delta)^{1/N}$ , to compute the required information. Primarily, the existing approximate turbulent methods, e.g., Refs. 7 and 8, assume a constant 1/7th power-law velocity profile. However, experimental results<sup>30</sup> show  $N$  to be a function of  $R_\theta$  and the effect of a variable  $N$  on the skin friction has been demonstrated.<sup>31</sup> In order to incorporate this effect, the analysis of Ref. 11 assumed a skin-friction relation as

$$C_f / 2 = c_1 (R_\theta)^{-q} \quad (15)$$

With compressibility effects again accounted for by Eckert's reference-enthalpy technique, the turbulent heating-rate expression is

$$\dot{q}_{w,t} = c_1 (R_{\theta,e})^{-q} (\rho^* / \rho_e) (\mu^* / \mu_e)^q \rho_e U_e \times (h_{aw} - h_w) (Pr_w)^{-0.4} \quad (16)$$

where  $\theta$  can be written as

$$\theta_t = \left( c_2 \int_0^s U_e \rho^* \mu^* r^{c_3} ds \right)^{c_4} / (\rho_e U_e r) \quad (17)$$

The coefficients and exponents ( $q$ ,  $c_1$ ,  $c_2$ ,  $c_3$ , and  $c_4$ ) in Eqs. (15-17) are functions of  $N$  and are given as

$$q = 2.0 / (N + 1.0) \quad (18)$$

$$c_1 = (1.0 / c_3)^{2N / (N+1)} [N / (N+1.0) (N+2.0)]^q \quad (19)$$

$$c_2 = (1.0 + q)c_1 \quad (20)$$

$$c_3 = 1.0 + q \quad (21)$$

$$c_4 = 1.0/c_3 \quad (22)$$

$$c_5 = 2.24333 + 0.93N \quad (23)$$

A curve fit of the axisymmetric nozzle-wall data<sup>30</sup> for  $N$  as a function of  $R_{\theta}$  yielded

$$N = 12.67 - 6.5 \log(R_{\theta,e}) + 1.21 [\log(R_{\theta,e})]^2 \quad (24)$$

and was used to calculate  $N$  in the present study.

Procedures for applying the heating methods to three-dimensional and variable-entropy flow conditions were also discussed in Ref. 11. For the purpose of this investigation, the pertinent results applicable to variable-entropy conditions are presented. As a result of inherent difficulties involved with applying mass balancing to three-dimensional flows and apparent discrepancies that result from applying approximate or classical boundary-layer methods to mass balancing in axisymmetric flows, the effect of variable entropy on the heat transfer was approximated by a somewhat different approach than mass balancing. An iterative process involving a known inviscid solution, the momentum equations [Eqs. (14) and (17)], and ratios of boundary-layer thickness to momentum thickness is used to determine the local flow conditions. Thus variable-entropy effects are accounted for locally by moving out in the inviscid flowfield a distance equal to the boundary-layer thickness. The inviscid properties at this location are used as the boundary-layer edge properties. The boundary-layer thickness to momentum thickness ratios were given<sup>11</sup> as

$$(\delta/\theta_L) = 5.55 \quad (25)$$

and

$$\left(\frac{\delta}{\theta}\right)_t = N + 1.0 + \left\{ \left[ \frac{N + 2.0}{N} \left( \frac{h_w}{h_{aw}} \right) + 1.0 \right] \times [1.0 + 1.29 P_r^{0.333} * \left( \frac{U_e^2}{2h_e} \right)] \right\} \quad (26)$$

## Results and Discussion

In this section, the validity of the thermodynamic correlations is determined by comparisons with equilibrium-air shock properties based on detailed chemistry calculations. The correlations have been incorporated in an approximate inviscid-nonradiating-flowfield analysis with convective heating capability, and resulting convective heat-transfer calculations are compared with corresponding VSL results. A quantitative assessment of the impact of several existing viscosity models on the convective heating rates computed by the VSL code is presented also.

The present correlation equations for  $C_h$  and  $C_T$ , in conjunction with the oblique-shock relations, the equation of state [Eq. (1)], and the temperature equation [Eq. (2)] provide a simple technique for rapidly computing postshock properties over a wide range of Earth entry conditions. The approximate results for the postshock static enthalpy, density, and temperature have been compared in Ref. 28 with the detailed calculations.<sup>25-27</sup> A typical result for the normalized postshock static enthalpy is shown in Fig. 3 as a function of the product  $U_\infty \sin \theta_s$  for a range of freestream pressures from  $2.0 \times 10^{-5}$  to  $1.1 \times 10^{-1}$  atm. The comparison of the approximate and detailed results is good. In general, discrepancies of less than 1% were noted for the enthalpy and pressure comparisons and less than 4% for density and temperature comparisons. The present correlations are noted to be applicable only to flowfield calculations.

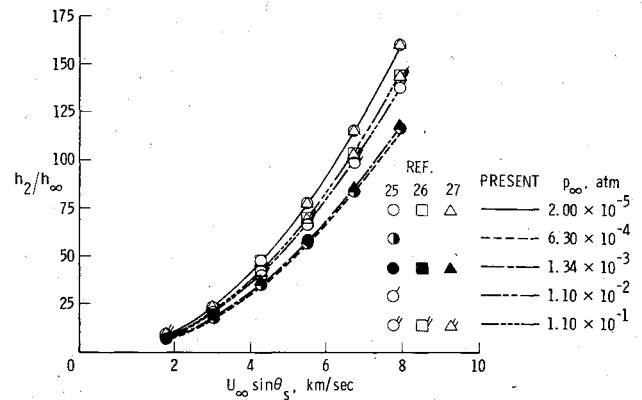


Fig. 3 Comparison of approximate and detailed normal shock solutions for static enthalpy.

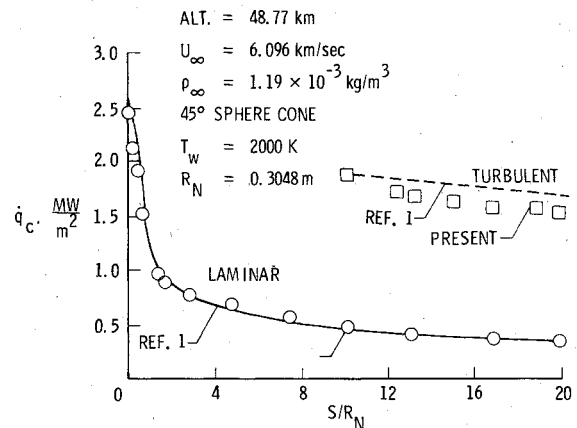


Fig. 4 Convective heat-transfer comparisons for a 45-deg sphere cone at ballistic entry conditions.

For the aerothermal planetary studies,<sup>12,18</sup> thermodynamic correlations, similar in form to the present equilibrium-air correlations, were incorporated in an inviscid-flowfield analysis with a convective heating capability for defining also the thermodynamic environment through the shock layer. The approximate flowfield analysis was demonstrated to yield heat-transfer results that are suitable for parametric or design calculations. Briefly, this flowfield technique is based on an inverse method of solution; i.e., analytic shock-shape equations are required such that the calculated body closely approximates the desired body configuration. Presently, two analytic expressions for bow shocks that are capable of generating body shapes closely approximating either spherically blunted cones or hyperboloids are used. The flowfield analysis is based on the Maslen<sup>32</sup> technique, which permits an independent evaluation of the pressure through the shock layer. Recently, a convective heat-transfer method<sup>11</sup> that accounts for variable-entropy flow conditions has been included in the flowfield calculations. Such approximate flowfield solutions provide reliable engineering calculations of the convective heat-transfer rates at Earth, Venusian, and outer-planet entry conditions.<sup>11</sup> The current equilibrium-air, thermodynamic correlations have been incorporated in this approximate flowfield code. Presently, the local thermodynamics are calculated along streamlines. The values of  $C_h$  and  $C_T$  [Eqs. (8) and (9)] are computed at postshock conditions where the streamline crosses the shock and are held constant along the respective streamlines. Certainly, other reference points could be used to evaluate  $C_h$  and  $C_T$  and the accuracy of the approach can be determined. Also, the present thermodynamic correlations could be incorporated in a flowfield code that does not require streamline information in its solution procedure.

Table 2 Impact of transport models on convective-power calculations<sup>a</sup>

Case	$U_\infty$ , km/s	$\rho_\infty$ , kg/m <sup>3</sup>	$T_w$ , K	Flow	Peng and Pindroh <sup>20</sup>	Armaly and Sutton <sup>21</sup>	Convective power with transport models			
							Yos <sup>22</sup>	Esch et al. <sup>23</sup>	Hansen <sup>24</sup>	Sutherland
I	6.096	$1.287 \times 10^{-4}$	2000	Laminar	14.94	14.62	...	14.70	13.38	13.45
II	3.048	$1.197 \times 10^{-3}$	2000	Laminar	2.82	2.75	...	2.70	2.58	2.62
III	6.096	$1.709 \times 10^{-2}$	2000	Laminar	148.06	143.95	144.46	146.16	129.98	128.19
IV	6.096	$1.709 \times 10^{-2}$	2000	Turbulent <sup>b</sup>	1252.47	1249.01	1244.84	1233.88	1230.15	1235.71
V	6.096	$1.709 \times 10^{-2}$	4000	Laminar	102.16	99.33	100.03	101.81	88.74	87.23
VI	6.096	$1.709 \times 10^{-2}$	4000	Turbulent <sup>b</sup>	752.52	744.98	742.67	740.53	703.82	706.53

<sup>a</sup> Power =  $\dot{q}_c dA$  MW. <sup>b</sup> Transition at  $S/R_N = 0.1$ .

Convective heating rates computed with the approximate flowfield method using the present equilibrium-air correlations have been compared<sup>28</sup> at freestream conditions that are representative of ballistic as well as Shuttle-like entries with corresponding VSL calculations.<sup>1</sup> The calculations are based on a 45-deg spherically blunted cone with a 0.3048-m nose radius and a 20-deg hyperboloid with a 0.0254-m nose radius. All calculations are for a 2000 K wall temperature, a 0-deg angle-of-attack condition, and employ the Sutherland viscosity law. Simple body geometries are selected for these heating-rate calculations since the purpose of these comparisons is to validate the use of the present equilibrium-air correlations in flowfield and heat-transfer calculations. In general, the results of the approximate laminar and turbulent calculations are found to be within 10-15% of the VSL results. For this paper, typical results for the 45-deg spherically blunt cone at a freestream velocity of 6.096 km/s are shown in Fig. 4. The turbulent heating rates were computed assuming instantaneous transition to turbulent flow at a local Reynolds number of  $1.0 \times 10^6$  based on laminar flow conditions. The computational time required for the approximate results is less than 45 s per case on the CDC 6600. This time is at least a factor of 10 faster than the time required for a corresponding VSL calculation. Thus the present equilibrium-air correlations can be incorporated in flowfield codes to provide a rapid, but reliable, method for predicting convective heating rates over re-entry vehicles at Earth entry conditions.

While the effect of differences in transport properties on the heat transfer is well documented, detailed transport property calculations for high-temperature air are not available. Thus it is difficult to select a "best" approximate transport model. As a matter of consistency in the heating-rate comparisons, the Sutherland viscosity law was used in the approximate heating and VSL methods. For the purpose of this investigation, a quantitative assessment of the impact of several existing viscosity models on the convective heat transfer is made. The viscosity models used in the present analysis are Peng and Pindroh,<sup>20</sup> Armaly and Sutton,<sup>21</sup> Yos,<sup>22</sup> Esch et al.,<sup>23</sup> Hansen,<sup>24</sup> and Sutherland. The procedures used to arrive at the mixture viscosity in Refs. 20-22 are considered to be more rigorous than those used in Refs. 23 and 24 and the Sutherland value. The ranges of freestream conditions, flow conditions, and wall temperatures used in the present assessment are presented in Table 2. The convective heat-transfer results are computed with the VSL<sup>1</sup> method over a 45-deg sphere cone with a 0.3048-m nose radius and a base-to-nose radius ratio of 14.4. For the calculations, the Prandtl number and Lewis number are assumed to be constant, with values of 0.72 and 1.4, respectively. The maximum temperature computed in the shock layer for these cases is less than 7000 K. In Table 2, the convecting heating results computed with various viscosity models are summarized in terms of the convective power,  $\dot{q}_c dA$ . Note that any differences in the convective-power results were observed also in a consistent manner for the heating-rate distributions over the entire body. The convective-power results based on the Yos<sup>22</sup>

model are presented at conditions for which tabulated viscosity data are available. For laminar-flow conditions and a 2000 K wall temperature (cases I, II, and III in Table 2), comparison of the convective-power calculations show that the maximum difference is about 10% for the six viscosity models. Furthermore, these results show that the heating predictions using the mixture viscosity values of Peng and Pindroh,<sup>20</sup> Armaly and Sutton,<sup>21</sup> Yos,<sup>22</sup> and Esch et al.<sup>23</sup> are in excellent agreement. A second grouping of convective results obtained with the Hansen<sup>24</sup> and Sutherland models are in good agreement also. The discrepancy in the laminar convective-power calculations is shown to be about 15% for a 4000 K wall temperature (case V). For turbulent flow and a 2000 K wall temperature, case IV, the convective power predicted by the six viscosity models is essentially the same. A similar comparison is obtained for a 4000 K wall temperature (case VI). In the VSL turbulent heating calculations, the turbulent viscosity dominates the molecular viscosity.

### Concluding Remarks

Engineering heating methods which have been verified by experiments and/or "benchmark" calculations are used in parametric or design studies to predict the aerodynamic heating rates about re-entry vehicles. The primary reason for using these methods is that these techniques provide significant reduction in computational time and computer storage requirements compared to the more detailed methods. Some aspects of the engineering methods that reduce the computer time and storage are thermodynamic and transport property correlations. An approximate flowfield technique employing such correlations has been demonstrated to provide rapid and reliable predictions for the aerodynamic heating rates about probes entering the atmospheres of the outer planets.

Thermodynamic correlations that are similar in form to those developed for the outer planets have been developed for equilibrium air. The thermodynamic correlations for both enthalpy and temperature in terms of density and pressure are applicable to a range of freestream velocities from 1.829 to 7.925 km/s and freestream pressures from  $2.0 \times 10^{-5}$  to  $1.0 \times 10^{-1}$  atm. The correlation equations and the methods used to develop the correlations are presented. The approximate postshock thermodynamic properties computed with the present correlations are validated by comparison with detailed equilibrium-air shock calculations. In general, the comparisons of the approximate and detailed calculated results yield discrepancies of less than 1% for enthalpy and pressure and less than 4% for density and temperature.

The thermodynamic correlations are incorporated in an approximate flowfield method with a convective heating capability. The heating method includes an option to approximate the effect of variable-entropy edge conditions on the heat transfer. Laminar and turbulent heating rates are computed about probes of simple geometry and at conditions representative of Shuttle- and ballistic-like entries. The comparison of the approximate heat-transfer results with

corresponding viscous-shock-layer (VSL) results is good. Thus the present thermodynamic correlations can be incorporated in approximate flowfield and heating methods to provide a reliable engineering technique for parametric and design calculations.

Currently, detailed transport calculations for high-temperature air are not available and a "best" approximate transport model cannot be determined easily. Consequently, the impact of existing viscosity models on the convective flux is demonstrated over a range of freestream conditions, flow conditions, and wall temperature values. For a wall temperature of 2000 K and laminar flow, the maximum difference in the convective power computed with the viscosity models is about 10%. At a wall temperature of 4000 K, the discrepancy is 15%. For turbulent flow and at both the 2000 and 4000 K wall temperature cases, the various viscosity models are shown to have an insignificant impact on the resulting convective-flux calculations.

### References

- <sup>1</sup>Moss, J. N., "Radiative Viscous-Shock-Layer Solutions with Coupled Ablation Injection," *AIAA Journal*, Vol. 14, Sept. 1976, pp. 1311-1317.
- <sup>2</sup>Kumar, A. and Graves, R. A. Jr., "Numerical Solution of the Viscous Hypersonic Flow Past Blunted Cones at Angle of Attack," *AIAA Journal*, Vol. 15, Aug. 1977, pp. 1061-1062.
- <sup>3</sup>Sutton, K. and Graves, R. A. Jr., "A General Stagnation-Point Convective-Heating Equation for Arbitrary Gas Mixtures," NASA TR R-376, 1971.
- <sup>4</sup>Lees, L., "Laminar Heat Transfer Over Blunt Bodies at Hypersonic Flight Speeds," *Jet Propulsion*, Vol. 26, April 1956, pp. 259-269, 274.
- <sup>5</sup>Cohen, N. B., "Boundary-Layer Similar Solutions and Correlation Equations for Laminar Heat-Transfer Distribution in Equilibrium Air at Velocities Up to 41,000 Feet Per Second," NASA TR R-118, 1961.
- <sup>6</sup>Zoby, E. V., "Approximate Relations for Laminar Heat Transfer and Shear Stress Functions in Equilibrium Dissociated Air," NASA TN D-4484, April 1968.
- <sup>7</sup>Phillips, R. L., "A Summary of Several Techniques Used in the Analysis of High Enthalpy Level, High Cooling Ratio Turbulent Boundary Layers on Blunt Bodies of Revolution," Ramo Wooldridge Corp., GM-TM-194, Sept. 1957.
- <sup>8</sup>Vaglio-Laurin, R., "Turbulent Heat Transfer on Blunt Nosed Bodies in Two-Dimensional and General Three-Dimensional Hypersonic Flow," *Journal of the Aerospace Sciences*, Vol. 27, Jan. 1960, pp. 27-36.
- <sup>9</sup>Cary, A. M. Jr. and Bertram, M. H., "Engineering Predictions of Turbulent Skin Friction and Heat Transfer in High Speed Flow," NASA TN D-7507, 1974.
- <sup>10</sup>Johnson, C. B. and Boney, L. R., "A Simple Integral Method for the Calculation of Real-Gas Turbulent Boundary Layers with Variable Edge Entropy," NASA TN D-6217, June 1971.
- <sup>11</sup>Zoby, E. V., Moss, J. N., and Sutton, K., "Approximate Convective-Heating Equations for Hypersonic Flows," *Journal of Spacecraft and Rockets*, Vol. 18, Jan.-Feb. 1981, pp. 64-70.
- <sup>12</sup>Zoby, E. V., Sutton, K., Olstad, W. B., and Moss, J. N., "An Approximate Inviscid Radiating Flow-Field Analysis for Outer Planet Entry Probes," *Progress in Astronautics and Aeronautics: Outer Planet Entry Heating and Thermal Protection*, Vol. 64, edited by R. Viskanta, AIAA, New York, 1979, pp. 42-64.
- <sup>13</sup>Cohen, N. B., "Correlation Formulas and Tables of Density and Some Transport Properties of Equilibrium Dissociating Air for Use in Solutions of the Boundary-Layer Equations," NASA TN D-194, Feb. 1960.
- <sup>14</sup>Garrett, L. B., Suttles, J. T., and Perkins, J. N., "A Modified Method of Integral Relations Approach to the Blunt-Body Equilibrium Air Flow Field, Including Comparisons with Inverse Solutions," NASA TN D-5434, Sept. 1969.
- <sup>15</sup>Olstad, W. B., "Nongrey Radiating Flow about Smooth Symmetric Bodies," *AIAA Journal*, Vol. 9, Jan. 1971, pp. 122-130.
- <sup>16</sup>Falanga, R. A. and Olstad, W. B., "An Approximate Inviscid Radiating Flow-Field Analysis for Sphere-Cone Venusian Entry Vehicles," AIAA Paper 74-758, July 1974.
- <sup>17</sup>Zoby, E. V., Gnoffo, P. A., and Graves, R. A. Jr., "Correlations for Determining Thermodynamic Properties of Hydrogen-Helium Gas Mixtures at Temperatures from 7000 to 35,000 K," NASA TN D-8262, Aug. 1976.
- <sup>18</sup>Zoby, E. V. and Moss, J. N., "Preliminary Thermal Analysis for Saturn Entry," AIAA Paper 80-0359, Jan. 1980.
- <sup>19</sup>Zoby, E. V., Graves, R. A. Jr., Moss, J. N., Simmonds, A., and Kumar, A., "Transport Property Correlations for H<sub>2</sub>-He Gas Mixtures at Temperatures of 1000-25,000 K," *AIAA Journal*, Vol. 18, April 1980, pp. 463-470.
- <sup>20</sup>Peng, T. C. and Pindroh, A. L., "An Improved Calculation of Gas Properties at High Temperatures: Air," Boeing Company, Document D2-11722, Feb. 1962.
- <sup>21</sup>Armaly, B. F. and Sutton, K., "Viscosity of Multicomponent Partially Ionized Gas Mixtures," AIAA Paper 80-1495, July 1980.
- <sup>22</sup>Yos, J. M., "Transport Properties of Nitrogen, Hydrogen, Oxygen, and Air to 30,000 K," Wright-Patterson Air Force Base, RAD-TM-63-7, March 1963.
- <sup>23</sup>Esch, D. D. et al., "Stagnation Region Heating of a Phenolic-Nylon Ablator During Return From Planetary Missions," NASA CR-112026, Sept. 1971.
- <sup>24</sup>Hansen, C. F., "Approximations for the Thermodynamic and Transport Properties of High-Temperature Air," NASA TR R-50, 1959.
- <sup>25</sup>Lewis, C. H. and Burgess, E. G. III, "Altitude-Velocity Table and Charts for Imperfect Air," AEDC-TDR-64-214, Jan. 1965.
- <sup>26</sup>Horton, T. E. and Menard, W. A., "A Program for Computing Shock-Tube Gasdynamics Properties," Tech. Rept. 32-1350, Contract NAS7-100, Jet Propulsion Lab., California Institute of Technology, Jan. 1969.
- <sup>27</sup>Nicolet, W. E., "User's Manual for the Generalized Radiation Transfer Code (RAD/EQUIL)," NASA CR-116353, Oct. 1969.
- <sup>28</sup>Zoby, E. V. and Moss, J. N., "Thermodynamic Equilibrium-Air Correlations for Flowfield Applications," AIAA Paper 81-0280, Jan. 1981.
- <sup>29</sup>Eckert, E. R. G., "Survey on Heat Transfer at High Speeds," U.S. Air Force, ARL 189, Dec. 1961.
- <sup>30</sup>Johnson, C. B. and Bushnell, D. M., "Power-Law Velocity-Profile-Exponent Variations with Reynolds Number, Wall Cooling, and Mach Number in a Turbulent Boundary Layer," NASA TN D-5753, April 1970.
- <sup>31</sup>Kutateladze, S. S. and Leont'ev, A. I., *Turbulent Boundary Layers in Compressible Gases*, Academic Press, Inc., New York, 1964.
- <sup>32</sup>Maslen, S. H., "Inviscid Hypersonic Flow Past Smooth Symmetric Bodies," *AIAA Journal*, Vol. 2, June 1964, pp. 1055-1061.